


© The Author(s), 2022. Published by Cambridge University Press for the Arizona Board of Regents on behalf of the University of Arizona. This is an Open Access article, distributed under the terms of the Creative Commons Attribution licence (<http://creativecommons.org/licenses/by/4.0/>), which permits unrestricted re-use, distribution and reproduction, provided the original article is properly cited.

TREE-RING-RADIOCARBON DATING PARAFFIN-CONSERVED CHARCOAL AT THE MISSISSIPPIAN CENTER OF KINCAID, ILLINOIS, USA

Nicholas V Kessler^{1*}  • Gregory L Hodgins² • Brian M Butler³ • Pulari S Kartha⁴ • Paul D Welch⁵ • Tamira K Brennan⁶

¹Laboratory of Tree-Ring Research and AMS Laboratory, University of Arizona, Tucson, Arizona, USA

²AMS Laboratory, University of Arizona, Tucson, Arizona, USA

³Center for Archaeological Investigations, Southern Illinois University, Carbondale, IL, USA

⁴Department of Chemistry and Biochemistry, University of Arizona, Tucson, AZ, USA

⁵Center for Archaeological Investigations, Southern Illinois University, Carbondale, IL, USA

⁶Illinois State Archaeological Survey, University of Illinois at Urbana-Champaign, Champaign, IL, USA

ABSTRACT. Archival charcoal tree-ring segments from the Mississippian center of Kincaid Mounds provide chronometric information for the history of this important site. However, charcoal recovered from Kincaid was originally treated with a paraffin consolidant, a once common practice in American archaeology. This paper presents data on the efficacy of a solvent pretreatment protocol and new wiggle-matched ¹⁴C dates from the largest mound (Mound 10) at Kincaid. FTIR and ¹⁴C analysis on known-age charcoal intentionally contaminated with paraffin, as well as archaeological material, show that a chloroform pretreatment is effective at removing paraffin contamination. Wiggle-matched cutting dates from the final construction episodes on Mound 10 at Kincaid, indicate that the mound was used in the late 1300s with the construction of a unique structure on the apex occurring around 1390. This study demonstrates the potential for museum collections of archaeological charcoal to contribute high-resolution chronological information despite past conservation practices that complicate ¹⁴C dating.

KEYWORDS: ¹⁴C, FTIR, Kincaid paraffin, wiggle-match.

INTRODUCTION

Archival wood and charcoal collections from the ancestral places of diverse Native American peoples in what is now the central and southeastern United States (known archaeologically as Mississippian), hold considerable importance as a source of chronometric information. While annual dendrochronological dating of archaeological wood and charcoal from the region remains challenging due to incomplete spatiotemporal coverage of long tree-ring chronologies, radiocarbon wiggle-matching provides a means to overcome these challenges by anchoring floating chronologies in time and providing archaeologists with high-resolution dates. If archival collections are to be utilized routinely for high-precision tree-ring based chronometry, challenges related to past conservation practices must be addressed. This paper outlines a study with the objective of providing high-resolution wiggle-matched dates for the terminal occupation of a Mississippian earthen mound from archival charcoal tree-ring segments. To accomplish this, we had to confront the issue of systematic contamination of charcoal by paraffin consolidants—a once widespread practice in American archaeology. This study was largely successful in removing paraffin contamination, and our dates provide high-resolution estimates for the era of peak sociopolitical complexity at the Kincaid Site.

History of Kincaid and Mound 10

Archaeological charcoal specimens analyzed here are the remains of architectural elements excavated in 1938 from the top of Mound 10 at the Kincaid site by the University of

*Corresponding author. Email: nvkessler@email.arizona.edu.

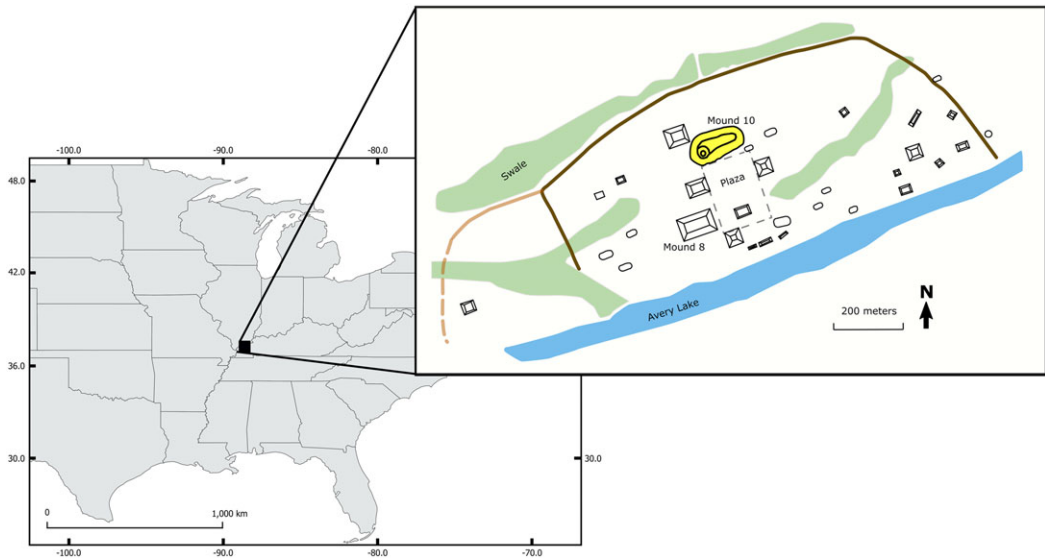


Figure 1 Location of the Kincaid site (inset) and a plan map of the site with mounds mentioned in the text labeled (Mound 10 is highlighted in yellow).

Chicago (Cole 1951). Kincaid was a Mississippian (AD 1000–1540, all dates are calendar years AD) political or religious center located on the floodplain of the lower Ohio River in what is now southern Illinois. Mound 10—situated north of the central plaza—is the largest monument at Kincaid (Figure 1). The earliest Mississippian village levels at the site (Early Kincaid) may date to the eleventh century (Butler et al. 2014), and ceramic cross-dating suggests the most intense occupation occurred between 1200 and 1300 (Middle Kincaid), when Kincaid is believed to have been a major socio-political and ceremonial center (Muller 1978). This interval likely witnessed the incorporation of diverse communities in distinct settlements adjacent to the core of Kincaid, the construction of the first palisade wall, mound building, and the emergence of marked material differentiation among households (Brennan 2014). Late in this period (Late Kincaid) or soon after, a massive expansion of the ritual and sociopolitical built landscape occurred coincident with a possible reduction of population and the physical footprint of the site (Brennan and Pursell 2020). This also traditionally demarcates the start of the decline phase at Kincaid (Butler 1991), and current syntheses suggest that the area was depopulated by the middle fifteenth century (Cobb and Butler 2002).

A few absolute dates for mound construction suggest that mound building associated with Middle Kincaid began around 1200. A single ^{14}C assay from the West Mound dates to between 1160 and 1280 and maize from Mound 4 dates to a similar time-period (Butler et al. 2011). A floating red cedar tree-ring chronology from a pre-mound level below Mound 4 has been recently anchored to after 1170 (Kessler et al. 2022). The timing of the subsequent expansion of the Kincaid built environment is informed by features buried under the edge of Mound 8 dating to ca. 1270–1430, a feature in the upper levels of West Mound dating to 1270–1400, a house on the main plaza dating to 1290–1400, as well as two dates from palisade walls in the same general time frame (Butler et al. 2011). Given the wide errors of the existing ceramic and ^{14}C chronologies, the order and timing of events within particular phases are unknown. This makes it impossible to discriminate short-term events or judge the tempo of the historical changes occurring at the site.

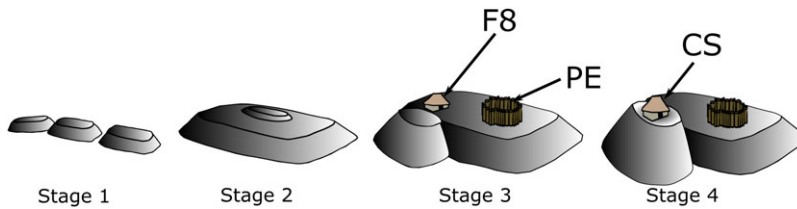


Figure 2 Schematic representation of the different construction stages inferred from archaeological evidence at Mound 10, and the features that yielded samples for this analysis (not to scale). Features labeled in Stage 3 refer to FVIII (F8), a structure built on the main platform adjacent to the first conical and to structures within a palisaded enclosure (PE). The feature labeled in Stage 4 is the structure (CS) built on top of the final conical platform level.

No independent dates exist for Mound 10 but the abundance of late Kincaid artifacts in the upper levels—the most thoroughly excavated part of the mound—suggest that it dates to the latter part of Kincaid history (Pursell 2016). Mound 10 consists of a long, truncated, platform mound and a conjoined conical platform. Excavators believe that Mound 10 was constructed in multiple stages with each stage dramatically altering its appearance (Emerson 1943) (Figure 2). Stage 1 involved the raising of a low truncate or three separate truncate mounds supporting at least one circular structure (Truncate Stratum IV and V in Cole 1951:95). Stage 2 saw the mound or mounds covered with fresh fill forming a long low truncate mound with a small platform on top but with no evidence of structures (Truncate Stratum III and II in Cole 1951:95). During Stage 3 successive fills were added to form a higher truncate supporting both palisaded and open access buildings (Truncate Stratum I in Cole 1951:95–96), at which time the conical mound was added with additional structures near its base (Conical Stratum III in Cole 1951:100). Finally, in Stage 4 the conical mound was heightened, and steps were added ascending the east side (Conical Stratum I in Cole 1951:100). At this stage, the conical portion of Mound 10 supported a single structure emplaced in a cuplike depression surrounded by an earthen berm or rampart (Pursell 2016:122). Charcoal samples analyzed in this study (Table 1) provide chronometric information directly related to the later stages of the mound construction, specifically Stages 3 and 4.

Paraffin Consolidants and Their Removal

The treatment of wood and charcoal with chemical consolidants is long-standing practice in archaeological conservation. Treatments range from surface coatings to substances that penetrate wood structure (Barbour 1990; Western 1969). For the past several decades, Acryloid B-72, Butvar 90 and 98, Polyethylene glycol (PEG), Klucel G, as well as newer natural polymers have been applied to dry or waterlogged wood and charcoal to preserve anatomical features, improve durability for transport and storage, and arrest biological degradation (Kaye 1995; Triantafyllou et al. 2010; Arista 2013; Walsh et al. 2014, 2017; Walsh-Korb and Avérous 2019). In the early and middle 20th century, natural and hydrocarbon waxes were also used to similar effect for both wood and charcoal. Paraffin wax in a molten state, and in solution with solvents, has been used to conserve a wide range of fragile materials for nearly a century in archaeology (Western 1969; Ramer 1979; Hatchfield and Koestler 1987; Schaefer and Mills 2017), and until fairly recently, paraffin-gasoline solution was widely used to preserve charred structural wood recovered from

Table 1 Summary of sample attributes for the archaeological charcoal from Mound 10 analyzed in this study.

Specimen ID	Species ¹	No. rings ²	Outer ring condition ³	Context	Building stage
mxo10-5B	C	36	vv	CS: Building at top of conical platform	Stage 4
mxo-10-7	Q	10	C	CS: Building at top of conical platform	Stage 4
mxo10-12	Q	37	vv	F8: Near Feature VIII, top of main platform	Stage 3
mxo10-28D	C	18	B	PE: Buildings in palisaded enclosure, top of main platform	Stage 3
mxo-10-75	Q	53	vv	F8: Near Feature VIII, top of main platform	Stage 3
mxo-10-173	C	60	v	PE: Buildings in palisaded enclosure, top of main platform	Stage 3
mxo-10-193	Jv	42	vv	F8: Near Feature VIII, top of main platform	Stage 3

Precontact archaeological sites across the U.S. for dendrochronological analysis (Towner 2015). The use of gasoline and paraffin is discouraged today because of risks associated with the fumes and the flammability of the samples, but some dendrochronologists continue to recommend chemical stabilization with substances such as polyethylene glycol for some samples (for example Koerner et al. 2009).

The major problem with chemical stabilization past and present is that it complicates ¹⁴C dating. This is significant as the AMS dating of sequential tree-rings (wiggle-matching) is contributing high-resolution dates to critical archaeological sequences. Wiggle-matching can be used in conjunction with dendrochronological analysis (Manning et al. 2010, 2014, 2016; Pearson et al. 2018, 2020; Grabner et al. 2021; Kessler et al. 2021), and in the context of broader ¹⁴C dating campaigns (Manning et al. 2018; Kessler et al. 2022) to provide high-precision dates for cultural deposits. The pervasiveness of paraffin-treated archaeological charcoal in U.S. museum collections is unknown, but may be widespread, considering the popularity of the method for much of the 20th century. If wiggle-matching is to be applied widely to archived wood originally collected for dendrochronological analysis, standard methods for removing paraffin contamination will be required.

Hawley-Bell Collection

The archaeological material for this study is housed in a large collection of charcoal and wood from Mississippian sites collected over 80 years ago in what we refer to as the Hawley-Bell collection. In the 1930s, archaeologists across North America were optimistically collecting tree-ring samples from buried contexts for submission to newly established tree-ring laboratories across the continent (for example Willey 1937; Hawley Senter 1938; Weakly 1943). The largest and most systematic project of this time outside of the Southwestern U.S. was undertaken by Florence Hawley and her former student Robert Bell. Their goal was to collect material for new tree-ring chronologies from the numerous Mississippian

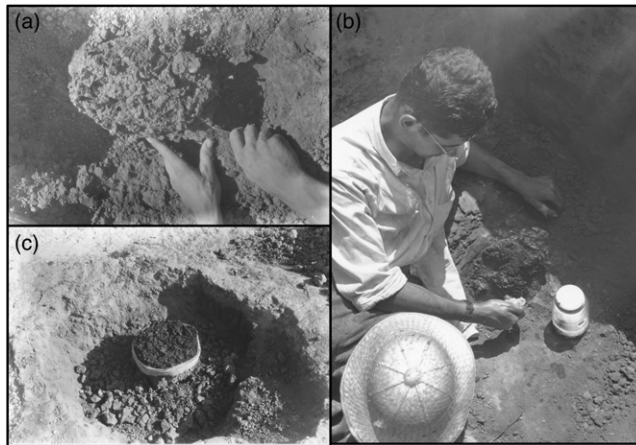


Figure 3 Steps for excavating and preserving charcoal remains at Kincaid during the University of Chicago excavations in 1937. In this sequence of photos, a post is excavated and cleaned of soil matrix (a), then the exposed post is soaked in paraffin solution (b), and the sample is wrapped in cotton string and allowed to dry and excavation continues (c). Joseph Caldwell is pictured in (b). (Courtesy Illinois State Museum, Illinois Legacy Collection, photographer: Frank Blackburn.)

towns and monumental centers in the Midwestern and Southeastern United States, the age of which was purely speculative (Stahle and Wolfman 1985; Nash and Copenheaver 2017).

The remains of Mississippian structures at these sites are preserved in most cases as burned and charred posts and beams. Charcoal is fragile and liable to disintegrate after drying out and being transported, so a method for stabilizing charcoal was developed by Hawley and collaborators. Correspondence between Bell, Hawley, and others in the field reveals a process of trial and error to adapt dendroarchaeological field methods to these contexts. The procedure that evolved required careful removal of soil adhering to charcoal as it is exposed in excavation, wrapping the sample in cotton gauze and string, and soaking the specimen in paraffin saturated gasoline (Figure 3). Based on our experience with wood preserved in this manner, paraffin is effective (although not perfectly so) at providing physical stability to charcoal specimens.

FTIR Analysis of Contaminated Charcoal

This study used Fourier-transform infrared spectroscopy (FTIR) to confirm the presence/absence of paraffin in archaeological charcoal prior to and after pretreatment. FTIR characterizes an array of molecular vibrations in a material via the measurement of the absorption intensity of middle infrared energy (Tasumi 2014). Though there are a wide variety of spectrometers, FTIR is unique in its speed and accuracy due to its use of an interferometer that allows all wavelengths of light to be measured simultaneously providing an average signal with low noise (Jaggi and Vij 2006). The absorbance or transmittance of the infrared spectrum produced by FTIR is plotted as a function of wavenumber (cm^{-1}) on the horizontal axis with relative intensity on the vertical axis, with intensity related to the proportional contribution of different chemical functional groups that are identified with

characteristic wavenumbers (Coates 2005:4). FTIR is commonly used to characterize the vapor and char of biofuel stocks and much of the literature on FTIR analysis of wood, lignin, and cellulose chars stems from this application (Collard and Blin 2014). In archaeology and material conservation sciences, FTIR is also useful when dealing with charcoal and wood. It has been used to discriminate between wood species (Traore et al. 2016, 2018), in wood provenance studies (Broda and Propescu 2019), and to detect trace contamination from chemical consolidants (Armitage et al. 2020). This study is an application of the latter, wherein we use FTIR analysis on archaeological and known-age charcoals to detect paraffin contamination and evaluate the efficacy of a ^{14}C pretreatment protocol.

Charcoal is often described simply as amorphous carbon, but its chemistry is actually much more complex due to variability induced by pyrolysis and diagenesis (Cohen-Ofri et al. 2006). Wood charcoal is predominantly derived from lignin and is composed of various organic compounds with the ratios of carbon to hydrogen and oxygen dependent on pyrolysis conditions that determine the degree to which different compounds are released (Collard and Blin 2014). The FTIR spectra of chars from whole wood and lignin tend to be dominated by a broad absorption band above wavenumber 3200 cm^{-1} due to the presence of O-H single bonds in hydroxyls in myriad contexts within the char, as well as multiple intense peaks between wavenumber $1800\text{--}1500\text{ cm}^{-1}$, attributed to the vibrations of carbonyls and aromatic rings (Sharma et al. 2004).

Paraffin is a saturated aliphatic compound whose absorption spectrum is dominated by the presence of long hydrocarbon chains. Specifically, a narrow and intense absorption band is observed at $2970\text{--}2950\text{ cm}^{-1}$ and $2880\text{--}2860\text{ cm}^{-1}$ from symmetric and asymmetric C-H stretching of methylene bonds (Coates 2000:5). In charcoal, however, IR (infrared) absorption at these wave numbers is minimal. Some studies observe very low IR absorption in charcoal between $3100\text{--}2860\text{ cm}^{-1}$, a band that reflects C-H stretching in endogenous hydrocarbons (Cao et al. 2013), although this is not detectable in all charcoals (Sharma et al. 2004; Trompowski et al. 2005). Importantly, for charcoals produced at combustion temperatures ranging from $300\text{--}1400^\circ\text{C}$, the intensity of IR absorption across $2970\text{--}2950\text{ cm}^{-1}$ is lower than the intensity of IR absorption in the region of O-H vibrations ($>3200\text{ cm}^{-1}$) (Sharma et al. 2004: Figure 7; Liu et al. 2008: Figure 7; Yu et al. 2012:7333; Cao et al. 2013:46). Based upon these observations we suggest that an increase in the IR intensity of the methylene band compared to the O-H band can provide an indicator of the presence of trace paraffin when the hydration level of the sample is controlled. We found this approach useful for interpreting ^{14}C results of paraffin contaminated charcoal.

METHODS AND MATERIALS

This study details the effects of a chloroform – hexane – ethanol – methanol – water solvent sequence for removing paraffin contamination from experimentally charred and contaminated wood as well as paraffin-conserved charcoal from archaeological contexts. The effect of the paraffin removal protocol was evaluated using FTIR and AMS dating.

Archaeological Samples

Charcoal from Mound 10 was recovered from structures enclosed by a palisade wall (context PE) and Feature VIII (F8), both constructed on mound Stage 3, and from the structure on top of the conical platform (CS) associated with Stage 4. The Mound 10 charcoal collection

consists of posts and roof poles made from true hickories (*Carya glabra* Sweet, *C. laciniosa* Michx. f., *C. ovata* K. Koch, or *C. tomentosa* Nutt.), white oak (*Quercus alba* L. *Q. stellata* Wang. *Q. muehlenbergii* Engelm, or *Q. macrocarpa* Michx.), and eastern red cedar (*Juniperus virginiana* L.) (see Table 1). Species were identified using wood anatomical features such as earlywood and latewood pore distribution, parenchyma morphology, ray thickness and density, and the presence/absence of tyloses using standard references (Core et al. 1979; Hoadley 1990). Of the true hickories and white oaks of southern Illinois, *C. ovata* and *Q. alba* are perhaps the most plentiful and grow mainly in upland hardwood forests (Fuller et al. 1955).

While the stratigraphic origin and general provenience of the samples are known, the context and architectural function of each charcoal specimen is only vaguely recorded. Based on the range of sizes it seems likely that they represent a mixture of roof poles, wall poles, and support posts. Charcoal selected for dating was preserved as complete and broken cross-sections. Sample mxo10-28D from Layer IB had remnants of bark demonstrating that the final growth ring was preserved and therefore likely dates the year of tree procurement (cutting date). Sample mxo10-7 from the top of the conical mound is interpreted as a small diameter pole, which based on the presence of a final growth ring across its entire circumference, also probably represents a cutting date. Sample mxo10-173 is subjectively considered a cutting date since its outermost surface resembled the contoured outer (waney), non-eroded, edge of a tree beneath the bark. The remainder of the samples lack indications of the true outermost ring and are interpreted as non-cutting dates with an unknown number of rings missing from their exteriors.

Charcoal Production

Known-age wood was obtained from bur oak (*Quercus macrocarpa*) trees sampled as cross-sections from north-central Kansas, USA in 2011 and archived at the Laboratory of Tree-Ring Research in Tucson, Arizona. A total of 1398 mg of wood was collected from rings dated as AD 1907. Samples were charred in an anoxic environment at 350°C for 60 min. While prehistoric hearths reached temperatures of over 600°C, researchers estimate that temperatures between 300–400 degrees results in the preservation of most archaeological botanical remains (Braadbaart et al. 2004; Lancelotti et al. 2010). Samples were packed in 9 mm diameter 325 mm long glass tubes stopped with quartz wool 50–60 mm from tube opening. Samples were placed under vacuum and pumped down to –27 Hg. Sample tubes were inserted into a tube furnace preheated to 350°C and left for 60 min while the temperature was monitored. Samples were allowed to cool under vacuum.

Paraffin Contamination

Subsamples of the known-age charcoal weighing between 60 to 120 mg were randomly selected for experimental paraffin contamination and pretreatment. A portion of each selected experimentally contaminated sample was reserved as an uncontaminated control. In a 150 mL beaker, Gulf Wax brand household paraffin was stirred into 50 mL of hexanes in ca. 1 g amounts until dissolution ceased at room temperature—or ca. 6 g of solid paraffin to 50 mL of hexanes for these trials. Charcoal pieces were then immersed in the hexane-paraffin solution until air bubbles were no longer observed emerging from wood vessels (about 5 min). The samples were then completely dried and sealed in scintillation vials.

Solvent Wash

^{14}C samples contaminated with paraffin wax require additional solvent washes prior to Acid-Base-Acid treatment (Brock et al. 2018; Bruhn et al. 2001). Recently, Armitage et al. (2020) demonstrated a simple procedure for removing paraffin contaminants from Neolithic-age charcoal-based pigments. Their trials involved three 15-min sonication rinses in 1 mL of chloroform followed by base treatment to remove humates. This treatment removed paraffin traces based on both spectral and ^{14}C analyses and was successful for both ground and consolidated charcoal with reported mass loss of 21–39%.

Our study adopted a chloroform wash modified from Armitage et al. (2020). Alternative methods were also evaluated in pretrials of this study and—while these methods proved effective—the chloroform protocol described below was both consistent and time efficient. Our final protocol consisted of first crushing approximately ~50–200 mg of a contaminated charcoal fragment to the consistency of coarse sand; this enabled the solution to penetrate the sample while still allowing easy handling and decanting. The crushed (non-homogenized) sample was then immersed in 5 mL chloroform inside a scintillation vial for a total of three hours in a sonication bath with the solution changed every 60 min. After decanting the third and final chloroform rinse, the sample was completely dried under a fume hood. The sample was then rinsed in successive solutions of hexanes, ethanol, methanol, and Type 1 ultrapure water for an hour in each solvent at 70°C, with the respective solutions changed three times. Rinsing in heated vials helps preserve our fragile material, but for more structurally sound samples the hexanes – ethanol – methanol – water washes could be accomplished using a Soxhlet apparatus. The samples were dried completely in an oven set to 50°C before ABA pretreatment described in the “ ^{14}C Analysis” section below.

FTIR Analysis

Samples at different stages in the trials were submitted to FTIR analysis to confirm the presence of paraffin in both archaeological and experimentally contaminated samples and to gauge the effects of different paraffin removal techniques. A Thermo Scientific Nicolet iS10 Smart FTIR device housed at the Arizona State Museum on the campus of the University of Arizona, Tucson was used for this study. Samples were compressed on a diamond window and spectra collected using ATR mode. Absorption was corrected for attenuated reflectance and atmospheric background. The paraffin used in the experimental treatments was compared to paraffin in a spectra library to confirm its spectral signature.

A simple diagnostic absorption intensity ratio was adopted in this study to classify paraffin contaminated specimens from uncontaminated ones. The relative absorbance ($R_{m/h}$) of the methyl/methylene band (~2970–2915 and 2880–2850 cm^{-1}) compared to the broad hydroxy band (~3600–3200 cm^{-1}) is quantified by the quotient of the maximum wavenumber intensities within the two respective bands. Other studies consistently find that the maximum hydroxy band intensity is higher than the methyl/methylene band in laboratory chars and charcoal, and so a $R_{m/h} > 1.00$ is used in this study as a first pass criterion for classifying samples as contaminated prior to ^{14}C dating. Admittedly, the interpretation of the O-H band is complicated by the water content of the sample, with wavenumber intensity at 3200–3600 cm^{-1} positively related to the humidity of the sample. However, at relatively low humidity (<50%) the effect of water on the O-H band intensity is muted (Deeyai et al. 2013: Figure 2; Celino et al. 2014: Figure 4). In this study, samples submitted to FTIR analysis were stored in sealed glass vials at both ambient indoor

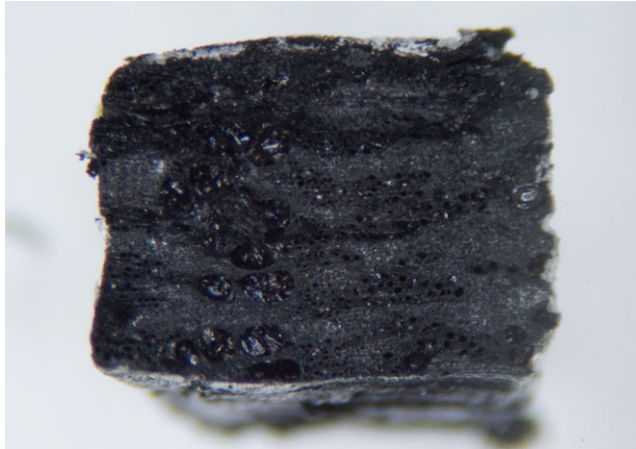


Figure 4 Known age oak charcoal experimentally contaminated with paraffin (140× magnification).

humidity (~25% in Tucson, AZ) and in a vacuum oven. No difference was detected in the wavenumber intensities of identical samples stored under the different conditions, and it is assumed that the hydration level of the samples in our study are sufficiently low to allow interpretation of the hydroxy band wavenumber intensity.

¹⁴C Analysis

All samples (whether treated with the solvent washes or not) were subjected to acid-base-acid treatment to remove inorganic carbonates and humates (Olsson 1980). Samples were soaked in 3 N HCl at 70°C and then rinsed to a neutral pH with Type 1 water. This was followed by the base step that involved immersion in 1.2 N NaOH at 70°C overnight and then additional NaOH rinses as warranted until no discoloration was observed in the NaOH solution indicating humate removal. When samples showed signs of dissolution, they were rinsed in the base solution at room temperature until a clear solution was obtained. Samples were then soaked in 3 N HCl at 70°C for one hour and rinsed in Type 1 water to neutralize pH and to remove absorbed CO₂.

Archaeological and known age samples were combusted, stable isotopic composition measured, and graphitized using an in-line EA-IRMS-AGE system consisting of a Vario ISOTOPE Select element analyzer coupled with an Elementar Isoprime PrecisIon mass spectrometer and IonPlus automated graphitization equipment. Radiocarbon measurements were performed on graphite targets at the Center for Applied Isotope Studies at the University of Georgia and radiocarbon content measured relative to SRM4990C, the Oxalic Acid II standard. Ten samples of archaeological charcoal were submitted to the University of California Irvine KECK Carbon Cycle Accelerator Mass Spectrometer Laboratory (UCIAMS), nine of which were for the purpose of replication. UCIAMS samples were combusted at 900°C in evacuated sealed quartz tubes in the presence of CuO oxidizer. Cryogenically purified CO₂ was reduced to graphite at 560°C with hydrogen and iron powder catalysts. Results are background subtracted and corrected for isotope fractionation. Calibrations were performed against the IntCal20 data set (Reimer et al. 2020), using OxCal v 4.4.4 (Bronk Ramsey 2009a; 2021). Replicate measurements were

compared using the `Difference()` function in OxCal. The mean calibrated date of the replicate samples (where the difference overlapped zero at 95.4% confidence) was calculated using the `R_Combine()` function. Archaeological samples were calibrated in wiggle-matching `D_sequence()` models based upon Bronk Ramsey et al. (2001). To account for the in-built age of non-cutting dates, the wiggle-matched posterior of each non-cutting date was calibrated in their stratigraphic sequence with OxCal “charcoal” outlier models (Bronk-Ramsey 2009b) or an empirical log-normal distribution for short ring segments from archaeological charcoal cross-sections provided in Kessler (2021) and the resulting models compared.

RESULTS AND DISCUSSION

Laboratory Contamination

Laboratory paraffin contamination produced charcoal samples with a waxy feel and white coatings visible on the surface and inside wood pores (Figure 4). This is similar to museum specimens known to have been conserved with paraffin. However, archaeological material initially *not* thought to been conserved with paraffin was revealed in pretrial FTIR analysis to contain probable paraffin residues. Pre-trial FTIR analysis also showed that interior rings may contain trace paraffin contamination despite the fact that outward signs of contamination are concentrated in the outer portion of the specimen. Therefore, while our laboratory contamination produced macroscopic and tactile characteristics consistent with paraffin-treated charcoal in museum collections, we do not consider visual or tactile clues to be definitive indicators of contamination.

Pretreatment with the solvent sequence eliminated outward indications of paraffin contamination for both known-age and archaeological charcoal samples. Mass loss during pretreatment averaged 33 percent (range = 29–40%) for known-age samples with the removal of paraffin contributing about 24 percent of this figure. The mass loss for archaeological samples averaged 64 percent (range = 33–97%). Base treatment for humate removal accounted for most of this loss and explains why the relatively fragile archaeological material exhibited much higher mass loss.

FTIR Analysis—Known Age Charcoal

Paraffin contamination produces a distinct FTIR spectra that helps identify it in charcoal. Table 2 summarizes characteristic wavenumber bands associated with each of the sample types in this study. As expected, the paraffin used to contaminate the known-age charcoal matches FTIR library spectra and is characterized by intense bands at $\sim 2920\text{ cm}^{-1}$ and $\sim 2850\text{ cm}^{-1}$ from C-H stretching of methylene, and these peaks dominate the spectra of paraffin-contaminated charcoal as well (Figure 5). Additional bands at $\sim 1470\text{ cm}^{-1}$ and $\sim 720\text{ cm}^{-1}$ observed in paraffin are due to C-H bending and rocking of methylene, consistent with the presence of hydrocarbons.

All known-aged charcoal samples show a broad hydroxy absorption band between 3400 cm^{-1} and 3200 cm^{-1} (Figure 6). A low intensity band around 2600 cm^{-1} indicates O-H stretching of H-bonded carboxylic acids (Trompowski et al. 2005). All laboratory-produced charcoal in this study exhibits a low intensity wavenumber peak around 1700 cm^{-1} from C=O stretching of carbonyl compounds. The intense absorption bands at $\sim 1590\text{ cm}^{-1}$ and $\sim 1508\text{ cm}^{-1}$ are

Table 2 Summary of wavenumber absorbance bands observed for different classes of charcoal in this study.

Wavenumber (cm ⁻¹)	Material	Vibration	Functional group attribution (reference)
3340–3193	C, U, T	O-H stretch	Hydroxy (1, 6)
2939–2917; 2854–2840	P, C, U, T	C-H stretch	Methylene (1, 5)
2625–2550	C, U, T	O-H stretching	H-bonded carboxylic acids (6)
1705–1693	C, U, T	C=O stretch	Unconjugated (>1700) and conjugated carbonyls (<1700) (ketone or carboxylic acids) (3, 4, 6, 7)
1592–1585; 1518–1507	C, U, T	C=C-C stretch	Aromatic rings (4)
1469	P, C	C-H bend	Methylene (1, 5)
1461–1421	C, U, T	C-H bend, C=C skeletal vibrations	Aliphatic or aromatic ring compound (1, 3, 5)
1332–1019	C, U, T	various C-O and C-H vibrations	Overlapping C-O groups (alcohols and phenol) and aromatic rings (1, 4)
824–673	C, U, T	C-H out-of-plane bending	Aromatic rings (3)
719–715	P, C	C-H rocking	Methylene (1, 5)

Material: P = paraffin, C = contaminated charcoal, U = uncontaminated charcoal, T = solvent-treated charcoal. References: Cao et al. 2013 (1), Coates 2000 (2), Patrova et al. 1994 (3), Sharma et al. 2008 (4), Stuart 2004 (5), Trompowski et al. 2005 (6), Yu et al. 2012 (7).

produced from aromatic ring vibrations with the higher intensity of the former band differentiating these hardwood samples from conifer species (Sharma et al. 2004).

For paraffin-contaminated charcoal, a band between ca. 1470–1430 cm⁻¹ overlaps methylene C-H bending but is also consistent with various combinations of C-C and C=C vibrations of aromatic rings and endogenous aliphatic compounds found in lignin (Pastorova et al. 1994; Sharma et al. 2004; Cao et al. 2013). That this same band is also present in uncontaminated charcoal (1461–1425 cm⁻¹), suggests this band is not diagnostic of paraffin contamination. A broad absorption band with multiple small peaks between ~825 cm⁻¹ and ~670 cm⁻¹ is observed in all charcoal samples and probably reflects C-H out-of-plane bending in aromatic rings (Pastorova et al. 1994). Within this region, a low intensity peak at ~715 cm⁻¹ occurs in contaminated samples and may correspond to the methylene C-H rocking from paraffin, but it is difficult to interpret small peaks in this region of the spectrum.

The two contaminated charcoal samples not subjected to solvent washes have $R_{m/h}$ values around 1.7 indicating significantly higher absorbance in the methylene band relative to the hydroxy band (Table 3). All known-age uncontaminated and contaminated solvent-treated charcoal samples have $R_{m/h} < 1$ (both averaging around 0.9), with the FTIR spectra closely similar to laboratory-produced wood, lignin, and cellulose chars analyzed in other studies

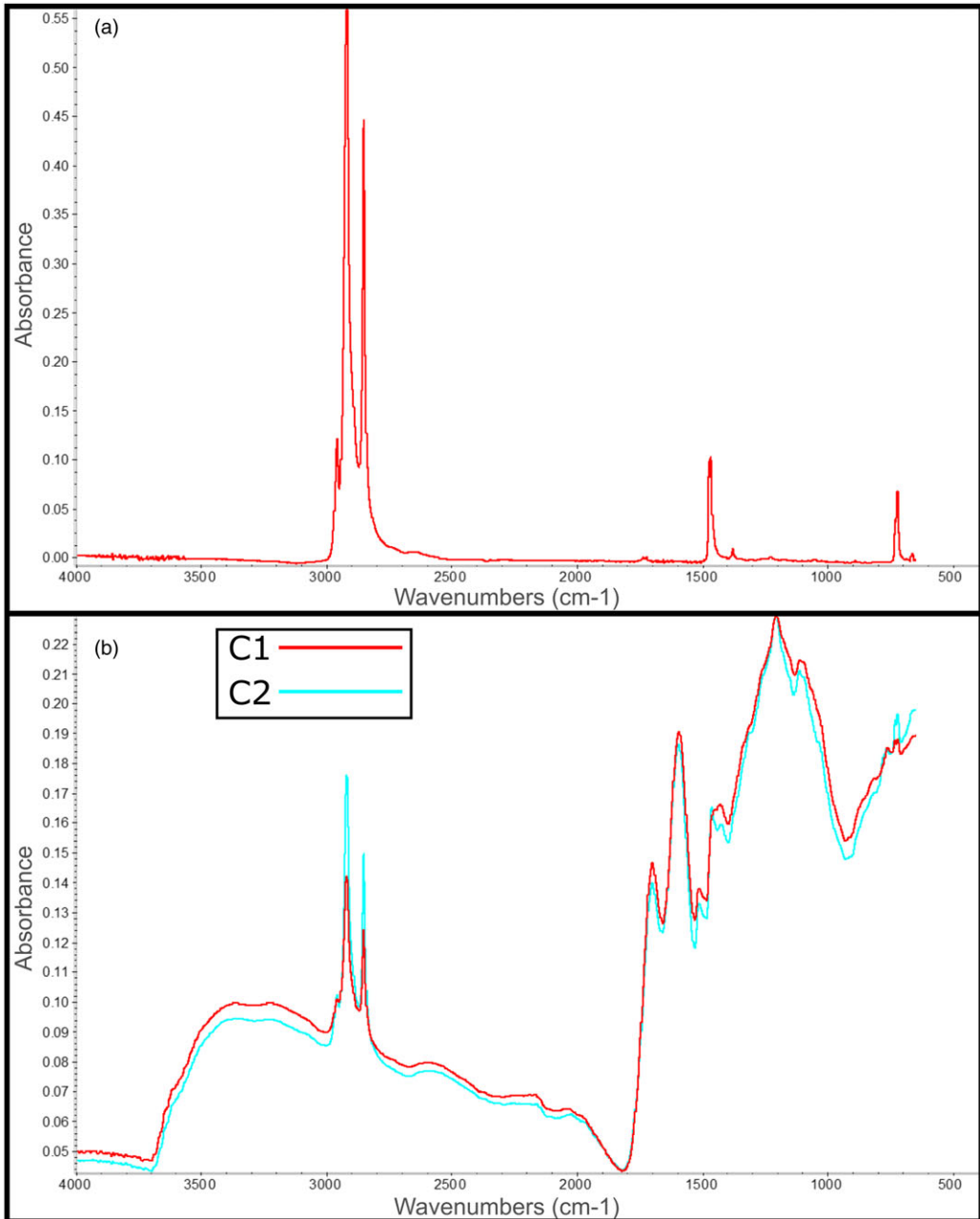


Figure 5 Pronounced methylene absorption bands are present in the FTIR spectra for paraffin wax (a) and known-age contaminated charcoal intentionally contaminated with paraffin (b).

(Sharma et al. 2004; Liu et al. 2008; Yu et al. 2012; Cao et al. 2013). This confirms our visual assessment of the FTIR spectra that the pretreatment protocol is effective at removing paraffin from lab-contaminated charcoal.

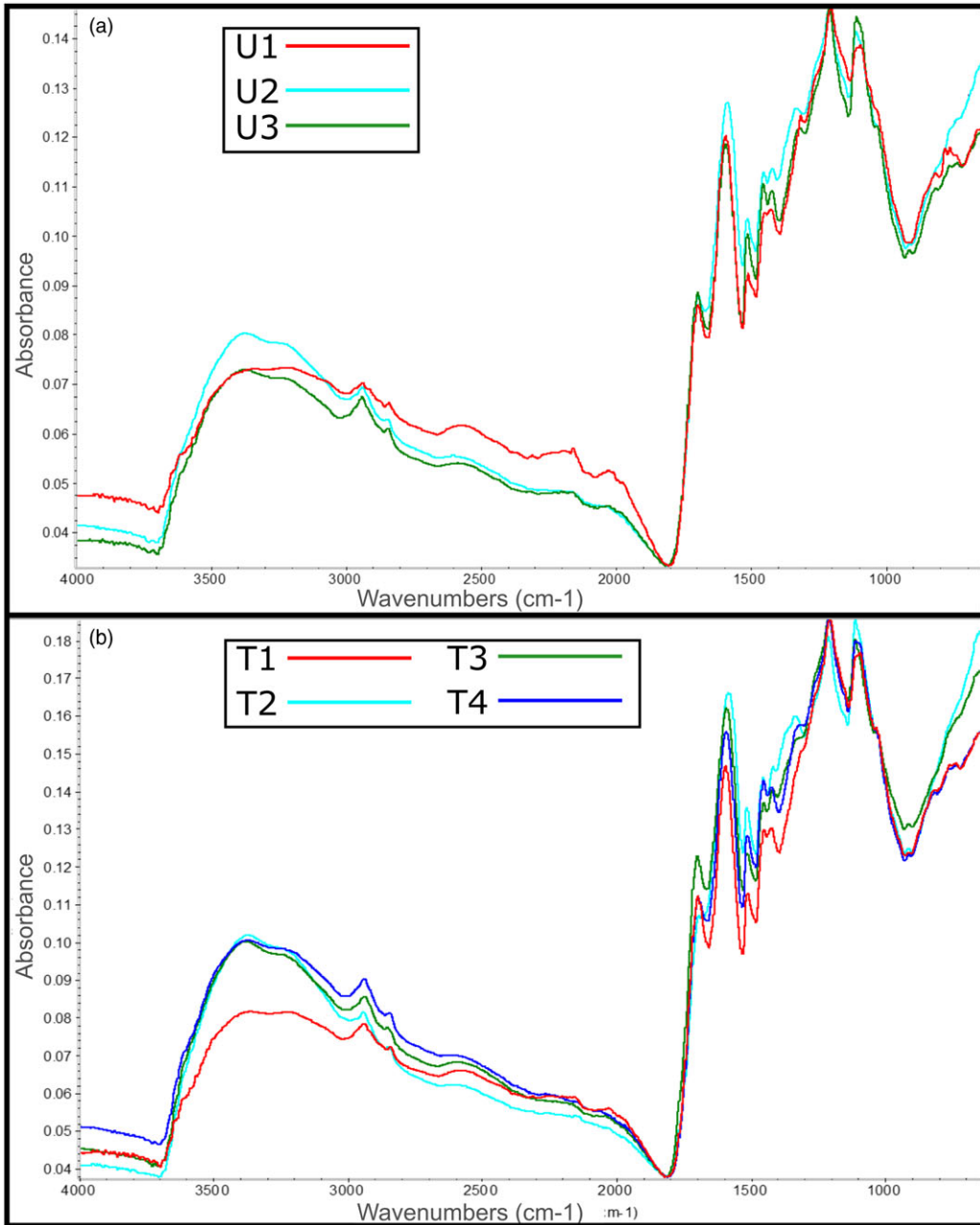


Figure 6 FTIR spectra of uncontaminated known-age charcoal (a) and intentionally contaminated known-age charcoal treated with a chloroform-hexanes-ethanol-methanol-water solvent sequence (b). Note that the methylene absorption band in (b) are similar in intensity compared to (a).

¹⁴C Analysis—Known Age Charcoal

A total of nine ¹⁴C dates were obtained on the known-age charcoal in this study are reported in Table 4. The effects of paraffin contamination have an unambiguous effect on the ¹⁴C ages of

Table 3 Relative absorbance intensity ($R_{m/h}$) of the hydroxy and methylene band of pretreated archaeological samples.

ID	Hydroxy	Methyl/methylene	$R_{m/h}$
Uncontaminated			
U1	0.080	0.070	0.87
U2	0.073	0.070	0.96
U3	0.072	0.069	0.96
Contaminated			
C1	0.101	0.142	1.41
C2	0.095	0.176	1.87
Treated			
T1	0.082	0.078	0.95
T2	0.101	0.086	0.85
T3	0.103	0.082	0.80
T4	0.103	0.091	0.88

charcoal in this study. ^{14}C dates on uncontaminated known-aged charcoal are obviously and significantly younger than the ^{14}C dates of the same charcoal contaminated by paraffin (Figure 7). The uncontaminated solvent-treated known-age charcoal returned calibrated ^{14}C dates with a combined calibrated date of 1826 ± 148 (2σ), consistent with their dendrochronologically determined true date of 1907 (Table 4). Paraffin-treated charcoal returned a combined calibrated date of 1246 ± 30 (2σ), showing that non-radioactive carbon is a larger constituent of contaminated samples than expected based on their true age. The fraction modern of the oldest measured ^{14}C age of the three uncontaminated samples is 0.9797 ± 0.006 (2σ) and does not overlap at 2σ the fraction modern of the youngest measured ^{14}C age of the two contaminated replicates at 0.9156 ± 0.0056 . Calculating the difference between contaminated and uncontaminated samples shows that paraffin consolidants in charcoal result in potential age offsets ranging from 427 to 694 years (95.4% posterior density). Contaminated known-age charcoal treated with the solvent protocol returned ^{14}C calibrated ages identical to the uncontaminated known-age material. The ^{14}C dating agrees with the FTIR results and show that the solvent treatment is effective at removing paraffin consolidants from lab-contaminated charcoal.

FTIR Analysis—Archaeological Charcoal

FTIR spectra from archaeological charcoal is similar to charcoal produced in the lab from known-aged wood. An assortment of archaeological charcoal specimens from the Hawley Bell collection not subjected to pretreatment all showed signs of paraffin contamination consistent with the FTIR spectra from both pure paraffin and contaminated charcoal (Figure 8a). This held true for archaeological samples not showing outward signs for paraffin contamination such as a visible residue or waxy texture, suggesting that paraffin consolidant was applied consistently to charcoal samples from Mound 10 in the Hawley-Bell collection.

FTIR scans of solvent-treated archaeological specimens from Mound 10 in the Hawley-Bell collection revealed absorption bands at 2600 cm^{-1} from O-H stretching on carboxylic acids, 1705 cm^{-1} from C=O stretching of unconjugated carbonyls (ketones), 1585 cm^{-1} from C-C

Table 4 ¹⁴C ages for known age charcoal samples.

Sample name	ID	Lab no.	$\Delta^{13}\text{C}$	Fraction modern	\pm	¹⁴ C age (BP)	\pm	Calibrated age (AD)	
								Min (95.4%)	Max (95.4%)
Uncontaminated									
pr01	U1	115083	-25.2	0.9797	0.003	165	25	1663	1950+
pr01-H	U2	115174	-25.4	0.9881	0.004	96	30	1685	1929
pr01-J	U3	115333	-25.3	0.9894	0.003	86	27	1691	1920
Contaminated									
pr01-D	C1	115087	-26.1	0.8809	0.005	1018	41	898	1157
pr01-I	C2	115175	-25.9	0.9156	0.003	708	25	1268	1381
Solvent-treated									
pr01-G	T1	115173	-25.5	0.9914	0.003	69	24	1694	1917
pr01-K	T2	115334	-25.3	0.9926	0.003	60	25	1694	1917
pr01-L	T3	115335	-25.3	0.9914	0.006	70	51	1679	1941
pr01-M	T4	115336	-25.5	0.9909	0.005	73	39	1683	1930

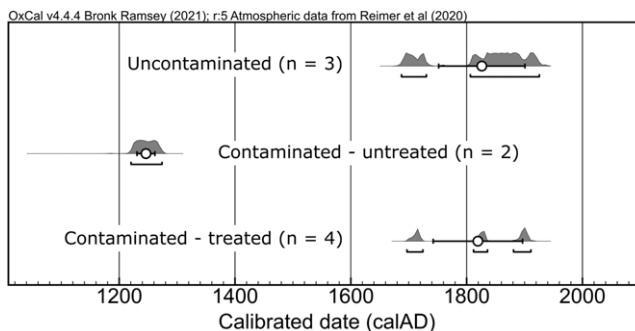


Figure 7 Posterior distributions of ^{14}C dated known age charcoal calibrated with the `R_Combine()` function in OxCal. Point and bars indicate the mean and error (1σ) respectively of the calibrated dates. Brackets span the 95.4% posterior range.

stretching of aromatic rings, and below 1400 cm^{-1} due to a variety of C-C, C-H, and C-O groups (Figure 8; see also Table 2). The broad absorption band across wavenumbers $3400\text{--}3200\text{ cm}^{-1}$ from O-H stretching was present across solvent-treated archaeological samples. As with lab-produced charcoal, low intensity absorption was present in archaeological samples at the methylene band around wavenumbers 2920 cm^{-1} and 2850 cm^{-1} . In only a single treated archaeological sample (ring 38 of mxo10-193) did this methylene absorption band exceed the hydroxy band ($R_{m/h} = 1.02$) (Table 5). This sample was flagged as potentially contaminated and was included in subsequent ^{14}C analysis to determine whether FTIR spectra could be used to screen pretreated charcoal for paraffin contamination in our study.

^{14}C Analysis—Archaeological Charcoal

This study produced 32 new ^{14}C dates from seven archaeological tree-ring segments that inform the late stages of construction on Mound 10 and help evaluate the paraffin removal protocol (Table 6). The ^{14}C measurement obtained from the suspect sample (AA11663) was ~ 280 ^{14}C years older than the next nearest ring in its segment. Calibrating this wiggle-match ring segment (mxo10-193) in an OxCal `Outlier_Model("RScaled", T(5), U(0,4), "r")` applied to the suspect date revealed an offset of 273 ± 27 (1σ) years. This confirms the identification based on $R_{m/h}$ that sample AA11663 contained traces of hydrocarbon contamination.

The contaminated sample was removed from the dataset and the replicate measurements were compared with the `Difference()` function. The 95.4% posterior density ranges of all the comparable measurements overlapped zero, and so replicates were combined using the `R_Combine()` function in the `D_Sequence()` models. The resulting wiggle-matched calibrated ages show generally good agreement with their relative placement in each ring sequence ($A > 60.0$) (Table 6, see also Supplement 1 for CQL code replicating all wiggle-match models). However, two dates—AA115661 and AA115664—were below the heuristic threshold of agreement. The ^{14}C age of the AA115661 is at least 27 years younger than its expected age based on its position in ring sequence mxo10-193, while the ^{14}C age of AA115664 is about 53 years younger than its replicate assay (UCIAMS259530) and is younger than the calibration data given its position in the ring sequence. In both cases, the

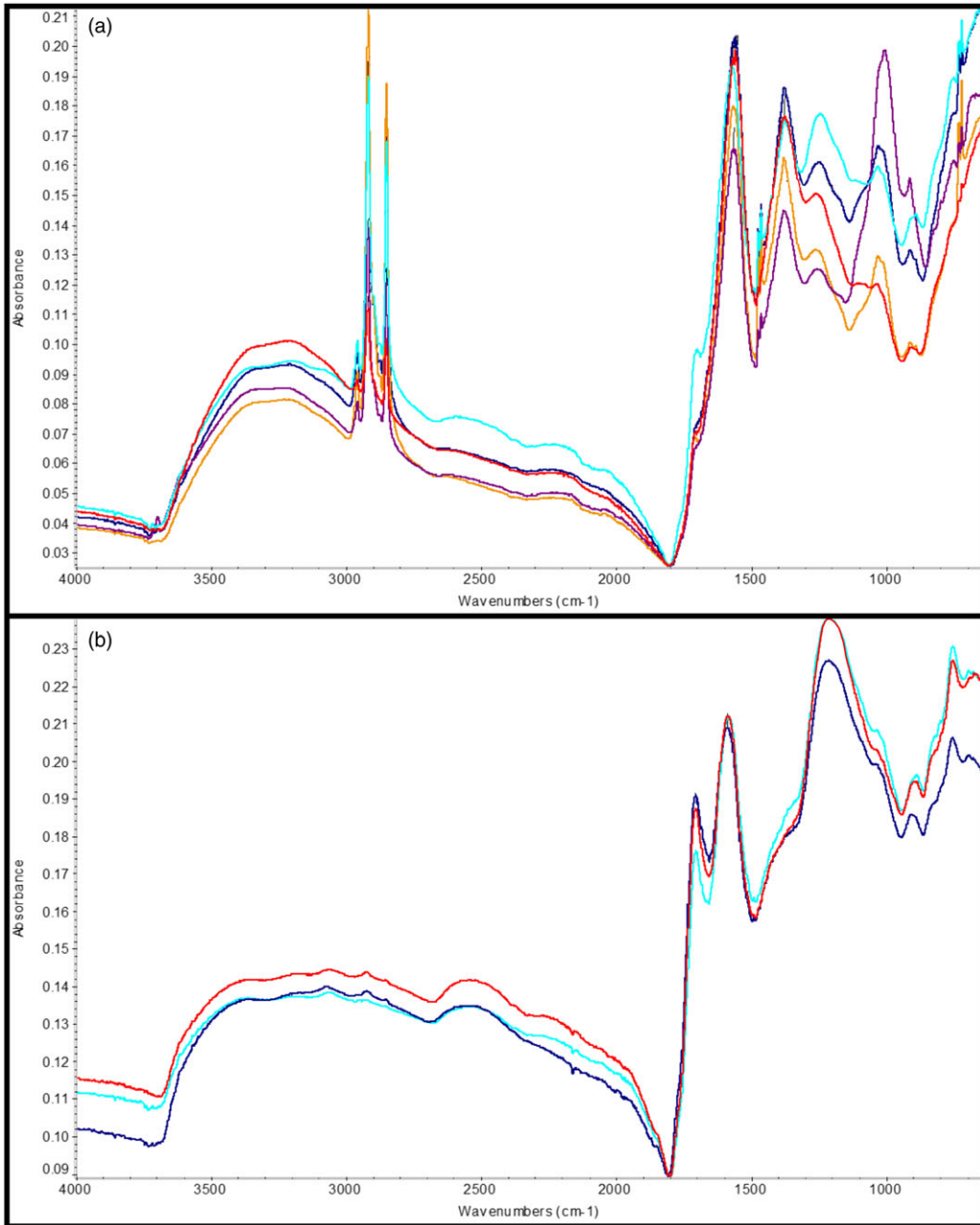


Figure 8 FTIR spectra of archaeological charcoal in the Hawley-Bell collection from a variety of contexts in Mound 10 prior to pretreatment (a), and pretreated charcoal from specimen mxo10-5B as an example of the change in the spectra due to pretreatment. Prior to treatment, pronounced methylene absorption bands indicate paraffin contamination panel (a) while the absence of intense absorption in this band indicates the absence of contaminants.

Table 5 Relative absorbance intensity ($R_{m/h}$) of the hydroxy and methylene absorption bands of pretreated archaeological samples.

Specimen ID	Ring no.	Hydroxy	Methylene	$R_{m/h}$
mxo10-5B	2	0.146	0.142	0.97
	14	0.139	0.134	0.96
	33	0.141	0.136	0.96
mxo10-7	1	0.134	0.132	0.99
	9	0.148	0.148	0.99
mxo10-12	1	0.122	0.115	0.94
	20	0.118	0.115	0.97
	36	0.022	0.021	0.98
mxo10-28	1	0.083	0.080	0.97
	17	0.078	0.076	0.97
mxo10-75	2	0.085	0.082	0.96
	11	0.088	0.083	0.94
	20	0.086	0.083	0.96
	40	0.088	0.083	0.94
mxo10-193	2	0.059	0.058	0.98
	8	0.069	0.059	0.85
	30	0.061	0.059	0.96
	38	0.056	0.057	1.02

combined agreement index of their respective $D_Sequence()$ models are acceptable ($A_{comb} > 60.0$) and re-running the models without the low agreement dates has only a small effect (± 2 years) on the modeled ages of the outermost rings. Therefore, these dates were retained in the $D_Sequence()$ models for the sake of completeness.

Wiggle-matched cutting dates from context PE place tree procurement at 1372 ± 36 (2σ) (mxo10-28D) and 1365 ± 8 (2σ) (mxo10-173) (Figure 9). The cutting date from context CS places tree procurement at 1346 ± 70 (2σ) (Figure 10) with the most likely posterior density ranges being 1303–1326 (52.1%) or 1378–1395 (34.0%). Wiggle-matched non-cutting dates from context F8 date to 1366 ± 10 (2σ) (mxo10-12D), 1388 ± 8 (2σ) (mxo10-75), 1382 ± 10 (2σ) (mxo10-193) and could indicate tree-procurement slightly later than context PE (accounting for missing rings from the non-cutting dates) (Figure 11).

Modeling the wiggle-matched dates in hypothetical sequences with two different outlier models to account for in-built age helps shed light on the most likely posterior dates for the final construction episodes on Mound 10 (see Methods and Material for in-built age correction). The wiggle-matched posterior date distributions, derived independently and described above, were saved as prior distributions to be input into each sequence model. Context F8 was thought to have been overlapped by the final conical fill (Emerson 1943), and so a plausible sequence of events places context F8 before context CS, with the construction and use of context PE possible at any time in the sequence. In other words, the model assumes only that construction material used in F8 is older than that used in CS, and that construction material for PE may overlap either phase temporally (see Supplement 2 for the archaeological sequence models).

Table 6 ¹⁴C ages for archaeological samples from Mound 10. Wiggle-matched dates in *italics* indicate that they represent an R_Combine () date from a pair of replicated ¹⁴C measurements.

Specimen ID	Ring no.	Context	Lab no.	$\Delta^{13}\text{C}$	¹⁴ C age (BP)	±	Calibrated age (AD)		Wiggle-matched age (AD)		Agreement
							Min (95.4%)	Max (95.4%)	Min (95.4%)	Max (95.4%)	
mxo10-5B	2	Conical strat	AA115670	-26.3	638	21	1290	1395	1290	1362	92.3
	14		AA115671	-26.0	603	21	1303	1402	1302	1374	97.5
	33		AA115672	-26.3	610	21	1302	1399	<i>1321</i>	<i>1393</i>	69
	33		UCIAMS259533	-26.3	615	20	1301	1399			
mxo-10-7	1	Conical strat	AA115668	-25.3	643	21	1288	1393	1294	1386	107
	9		AA115669	-32.9	552	21	1323	1425	<i>1302</i>	<i>1394</i>	<i>104.9</i>
	9		UCIAMS259532	-32.9	665	15	1282	1388			
mxo10-12	0	Palisade complex	AA115673	-26.2	556	21	1324	1423	<i>1320</i>	<i>1341</i>	<i>110.2</i>
	0		UCIAMS259534	-26.2	615	20	1301	1399			
	20		AA115674	-26.8	568	21	1321	1420	1339	1360	90.2
	36		AA115727	-26.7	680	21	1278	1387	<i>1357</i>	<i>1378</i>	<i>107</i>
	36		UCIAMS259535	-26.7	665	15	1282	1388			
mxo10-228D	1	Palisade complex	AA115676	-26.1	643	21	1288	1393	1281	1369	80.3
	17		AA115677	-26.0	694	21	1276	1381	<i>11297</i>	<i>1385</i>	<i>64</i>
	17		UCIAMS259536	-26.0	675	15	1281	1385			
mxo-10-75	2	Palisade complex	AA115664	-26.3	522	21	1398	1438	<i>1326</i>	<i>1341</i>	<i>54.4</i>
	2		UCIAMS259530	-26.3	575	15	1321	1410			
	11		AA115665	-28.1	589	21	1306	1407	1335	1350	126.8
	20		AA115666	-27.1	580	21	1309	1410	1344	1359	104.9
	40		AA115667	-27.6	626	21	1298	1396	<i>1364</i>	<i>1379</i>	<i>127</i>
	40		UCIAMS259531	-27.6	670	15	1281	1386			

(Continued)

Table 6 (Continued)

Specimen ID	Ring no.	Context	Lab no.	$\Delta^{13}\text{C}$	^{14}C age (BP)	\pm	Calibrated age (AD)		Wiggle-matched age (AD)		Agreement
							Min (95.4%)	Max (95.4%)	Min (95.4%)	Max (95.4%)	
mxo-10-173	9	Palisade complex	AA115678	-26.6	635	21	1292	1395	1306	1321	119.3
	19		115679R	-25.6	613	21	1301	1398	1316	1331	113.6
	30		AA115679	-26.0	533	21	1304	1404	1327	1342	107.9
	50		AA115680	-26.4	589	21	1306	1407	1347	1362	100
	59		UCIAMS259537	-26.4	650	15	1290	1390	1356	1371	89
mxo-10-193	0	F VIII	AA115660	-24.0	534	21	1321	1408	<i>1331</i>	<i>1349</i>	<i>116.1</i>
	0		UCIAMS259528	-24.0	620	20	1300	1398			
	8		AA115661	-23.2	553	21	1339	1357	1339	1357	47.9
	30		AA115662	-23.2	633	21	1294	1395	<i>1362</i>	<i>1379</i>	<i>112.6</i>
	30		UCIAMS259529	-23.2	675	15	1281	1385			
	38		AA115663	-24.0	931	22	1035	1165	Excluded from model		

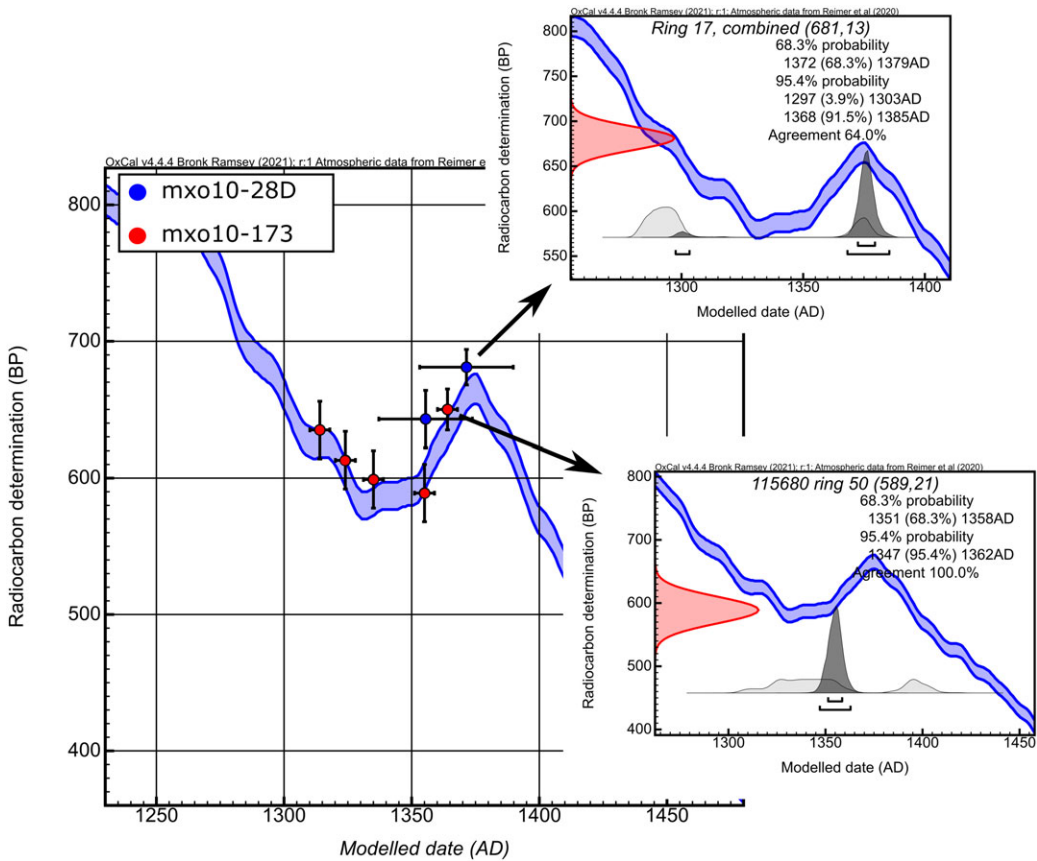


Figure 9 Wiggle-matched dates from `D_Sequence()` models on tree-ring segments from structures in the palisade enclosure (PE) on Stage 3 of Mound 10. Points represented the mean ¹⁴C and posterior dates and bars represent the 1σ range.

The model outputs are substantially similar regardless of the outlier model employed. The “empirical” outlier formulation results in higher model agreement ($A_{\text{model}} = 94.2$) compared to the “charcoal” outlier ($A_{\text{model}} = 76.4$) and the use of the former outlier results in wider posterior distributions suggesting it may provide somewhat more conservative age estimates (Figure 12), and so the results from the sequence employing the “empirical” outlier will be discussed further.

The prior information for the relative timing of F8 construction constrains the cutting date from context CS to the latter time period in its posterior density range or 1387 ± 8 (2σ) (the outlier model was not applied to cutting dates). The outlier model shifts a non-cutting date in context F8 to a younger age, and the Bayesian sequence suggests that construction of this context took place around 1381 ± 14 (2σ) based on the pooled mean and standard deviation of the three dates. The two sigma error ranges for the age estimate of F8 overlaps the cutting dates from context PE, which are unchanged in the sequence. These age estimates show that the palisaded enclosure (PE), the structure near the base of the conical (F8), and the structure on top of the conical platform

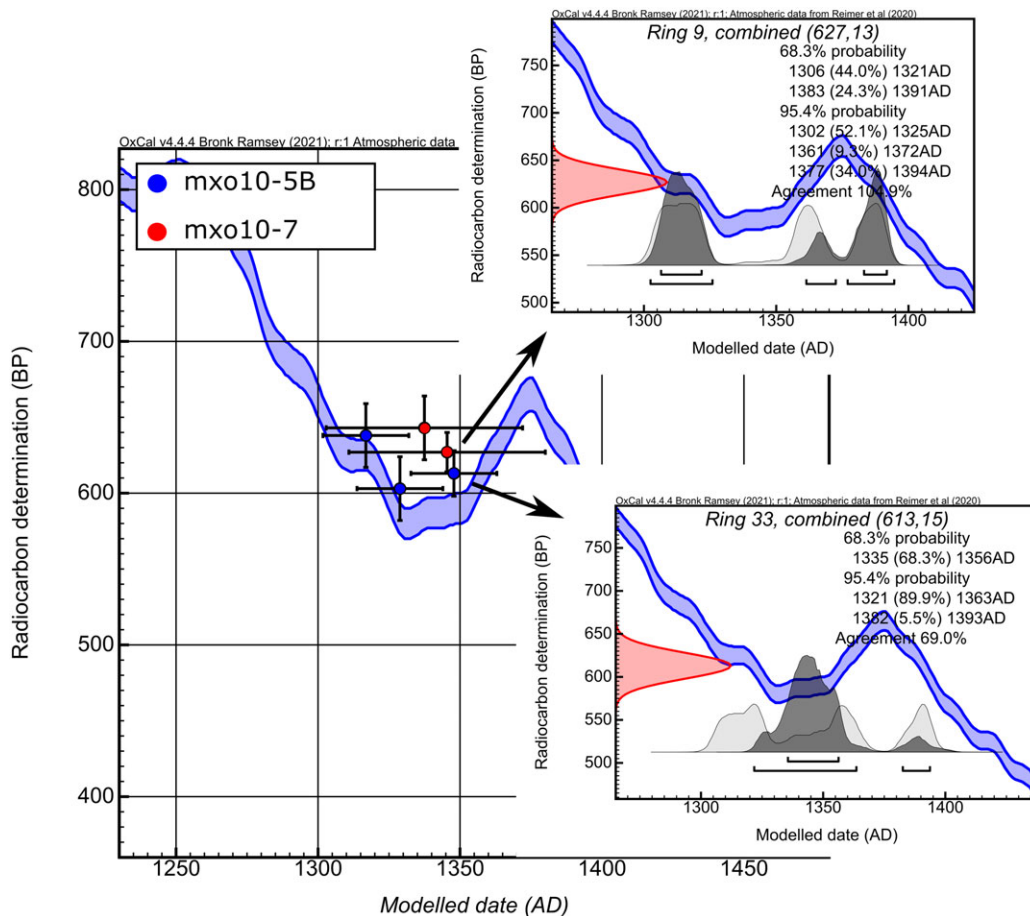


Figure 10 Wiggle-matched dates from *D_Sequence()* models on tree-ring segments from the structure on the top of the conical platform (CS) of Stage 4 of Mound 10. Points represented the mean ¹⁴C and posterior dates and bars represent the 1σ range.

(CS) may be contemporaneous constructions with the age ranges for the cutting dates from PE overlapping the cutting date from CS, and in any case, certainly represent a short time frame. An interval query for the F8-CS sequence shows that these dates represent a duration of no more than 26 years (95.4% posterior density). This indicates that the end of Stage 3 and the beginning of Stage 4 are separated by no more than a single generation and may have been coeval.

CONCLUSIONS

This study achieved a number of important results. The solvent treatment employed here completely removed traces of paraffin contamination from 95% of archaeological material, and from 100% of experimentally contaminated samples. FTIR analysis is a viable means for screening samples for paraffin (or other hydrocarbon) contamination prior to ¹⁴C analysis as the methylene peak produced by paraffin is easily identifiable. In our case study, the ratio of the absorbance intensity of the methylene and hydroxy bands (*R_{m/h}*)

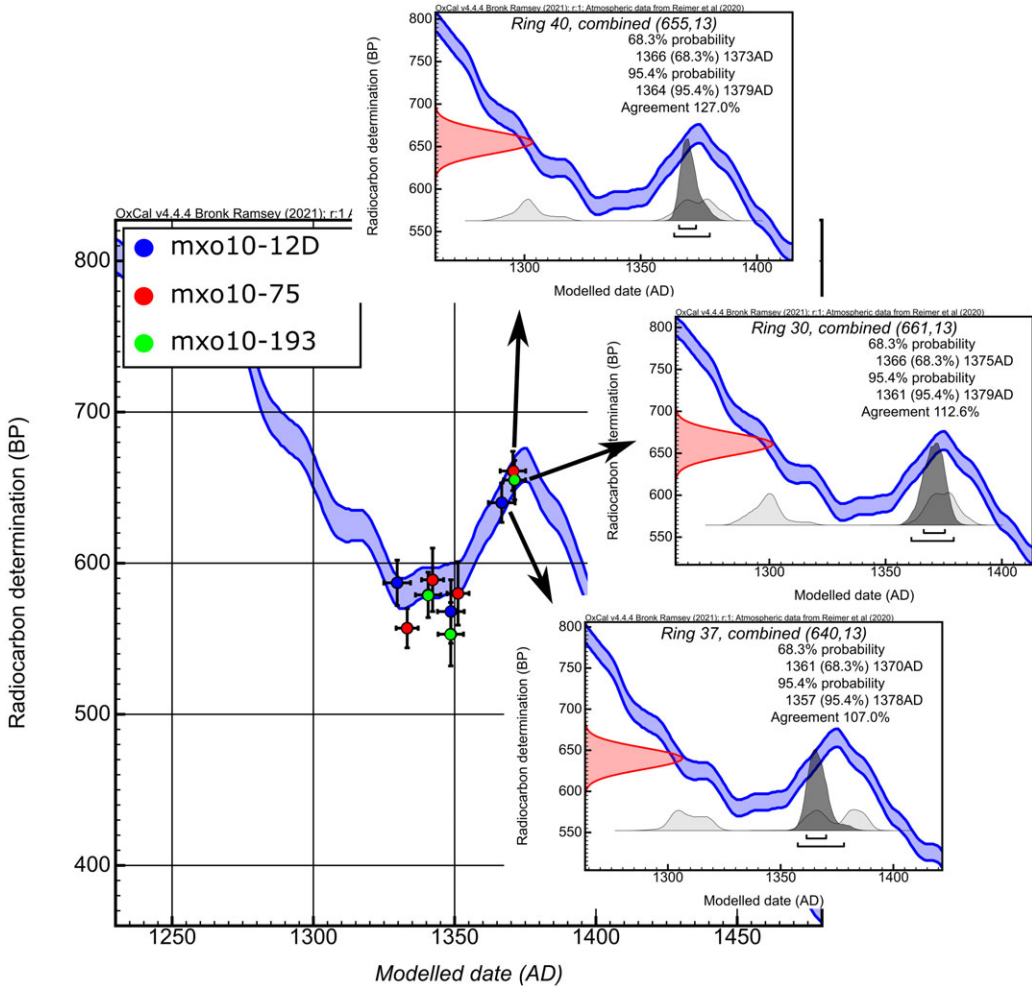


Figure 11 Wiggle-matched dates from *D_Sequence()* models on tree-ring segments from structures near FVIII (F8) on Stage 3 of Mound 10. Points represented the mean ¹⁴C and posterior dates and bars represent the 1σ range.

predicted the presence of contamination in the single archaeological sample in which pretreatment failed to remove all paraffin. The hydration level of the sample will affect the validity of this metric, and the fact that this analysis was conducted in Tucson, Arizona is not immaterial to our interpretation. However, for samples stored and analyzed at similar low humidity levels, the relative absorbance intensity of the methylene and hydroxy bands could be a useful metric for interpreting ¹⁴C offsets in cases where contamination is possible but uncertain.

Dates from final architectural contexts on Mound 10 are remarkably consistent and point to final construction on the main platform mound (Stage 3) beginning no earlier than the 1340s. The dates for the structure (context CS) built on the apex of the conical platform (Stage 4) indicate it was constructed around 1390 and probably within a generation of the completion of Stage 3. While the end boundary inferred from this dataset alone does not

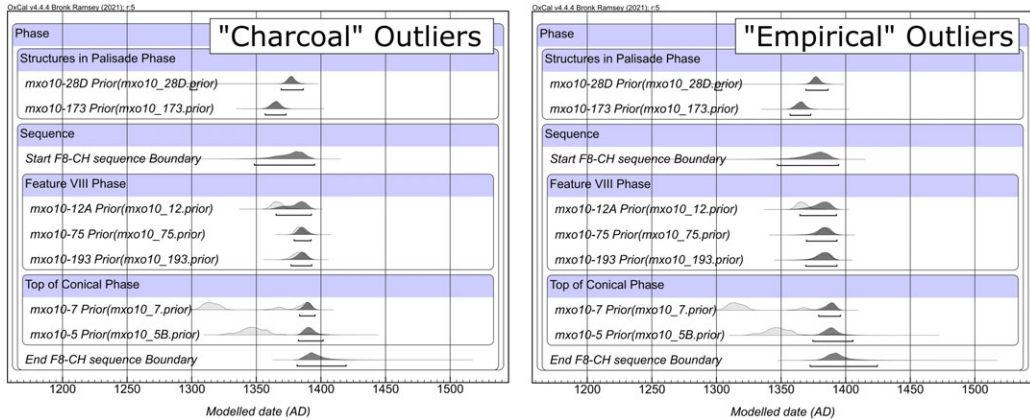


Figure 12 Posterior date distributions of the outmost rings of each wiggle-matched ring segment in the hypothetical construction sequence. At left, results from the sequence were the “charcoal” outlier model (Bronk Ramsey 2009) was used to account for potential in-built age of non-cutting dates. At right, results from sequence were an “empirical” outlier model (Kessler 2021) was used to account for potential in-built age of non-cutting dates.

allow a precise estimate for the terminal use of Mound 10, in light of the consensus view that Kincaid was unoccupied by the middle fifteenth century, events surrounding Stage 4 of Mound 10 probably occurred in the final generation or two of Kincaid occupation.

The resolution of this reconstruction is enabled by seven wiggle-matched dates on short (≤ 60 rings) charcoal tree-ring segments, three of which are cutting dates. The internal consistency of these dates and their coherency with the known cultural chronology of Kincaid supports the efficacy of the solvent treatment employed in the study. Obtaining high-resolution dates from short ring segments in archival, paraffin-conserved charcoal is an important finding for Mississippian archaeology because it demonstrates how this material can contribute to new high-resolution regional histories.

ACKNOWLEDGMENTS

Funding for this study came from the National Science Foundation (Award No. 2020313). Todd Lange, Li Cheng, and John Southon are thanked for their assistance with ^{14}C analysis. We are grateful to Peter Brewer, Kota Fleming, and archival staff at the Laboratory of Tree-Ring Research for cataloging the Hawley Bell collection and their help with accessing the material analyzed in this study. Two anonymous reviewers are greatly thanked for their attention to this manuscript and comments that improved the final work.

SUPPLEMENTARY MATERIAL

To view supplementary material for this article, please visit <https://doi.org/10.1017/RDC.2022.84>

REFERENCES

- Arista J. 2013. The effect of consolidation on the anatomical structure of floated charcoal remains at Kaman-Kalehöyük. *AAS*. XVII: 67–72.
- Armitage RA, Bueno-Ramírez P, de Balbín-Behrmann R, Martineau R, Carrera-Ramírez F, Fairchild T, Southon J. 2020. Charcoal-painted images from the French Neolithic Villevenard hypogea: an experimental protocol for radiocarbon dating of conserved and in situ carbon with consolidant contamination. *Archaeological and Anthropological Sciences*. 12:1–16.
- Barbour RJ. 1990. Treatments for waterlogged and dry archaeological wood. In: Rowell RM, Barbour RJ, editors. *Archaeological wood: properties, chemistry, and preservation*. Vol. 225. Washington D.C.: American Chemical Society. (*Advances in Chemistry*). p. 177–192.
- Braadbaart F, Boon JJ, van der Horst J, van Bergen PF. 2004. Laboratory simulations of the transformation of peas as a result of heating: the change of the molecular composition by DTMS. *Journal of Analytical and Applied Pyrolysis*. 71(2):997–1026.
- Brennan T K. 2014. Mississippian community making through everyday items at Kincaid Mounds [PhD dissertation]. Carbondale: Southern Illinois University.
- Brock F, Dee M, Hughes A, Snoeck C, Staff R, Bronk Ramsey C. 2018. Testing the effectiveness of protocols for removal of common conservation treatments for radiocarbon dating. *Radiocarbon* 60(1):35–50.
- Broda M, Popescu C-M. 2019. Natural decay of archaeological oak wood versus artificial degradation processes—an FT-IR spectroscopy and X-ray diffraction study. *Spectrochimica Acta Part A: Molecular and Biomolecular Spectroscopy* 209:280–287.
- Bronk Ramsey C. 2009a. Bayesian analysis of radiocarbon dates. *Radiocarbon* 51(1):337–360. doi: [10.1017/S0033822200033865](https://doi.org/10.1017/S0033822200033865).
- Bronk Ramsey C. 2009b. Dealing with outliers and offsets in radiocarbon dating. *Radiocarbon* 51(3):1023–1045. doi: [10.1017/S0033822200034093](https://doi.org/10.1017/S0033822200034093).
- Bronk Ramsey C. 2021. Analysis operations and models. Web document accessed 2021 Mar 10, <https://c14.arch.ox.ac.uk/oxcal/OxCal.html>.
- Bronk Ramsey C, van der Plicht JH, Weninger B. 2001. “Wiggle matching” radiocarbon dates. *Radiocarbon*. 43(2A):381–389. doi: [10.1017/S0033822200038248](https://doi.org/10.1017/S0033822200038248).
- Bruhn F, Duhr A, Grootes PM, Mintrop A, Nadeau M-J. 2001. Chemical removal of conservation substances by “soxhlet”-type extraction. *Radiocarbon* 43(2A):229–237.
- Butler B M. 1991. Kincaid revisited: the Mississippian sequence in the Lower Ohio Valley. In: Emerson T E, Lewis RB, editors. *Cahokia and the Hinterlands: Middle Mississippian Cultures of the Midwest*. Urbana: University of Illinois Press. p. 264–273.
- Butler B M, Welch PD, Brennan T K, Pursell CCO. 2014. Kincaid in the new century—recent investigations of a prehistoric Illinois metropolis. Web document, accessed 2020 Jan 30, https://cola.siu.edu/anthro/_common/documents/courses-and-field-schools/kincaid-in-the-new-century.pdf.
- Butler BM, Clay RB, Hargrave ML, Peterson SD, Schwegman JE, Schwegman JA, Welch PD. 2011. A new look at Kincaid: magnetic survey of a large Mississippian town. *Southeastern Archaeology* 30(1):20–37.
- Cao J, Xiao G, Xu X, Shen D, Jin B. 2013. Study on carbonization of lignin by TG-FTIR and high-temperature carbonization reactor. *Fuel Processing Technology* 106:41–47.
- Céline A, Gonçalves O, Jacquemin F, Fréour S. 2014. Qualitative and quantitative assessment of water sorption in natural fibres using ATR-FTIR spectroscopy. *Carbohydrate Polymers* 101: 163–170.
- Coates J. 2000. Interpretation of infrared spectra, a practical approach. In: Myers RA, editor. *Encyclopedia of Analytical Chemistry*. Chichester, United Kingdom: John Wiley & Sons.
- Cobb CR, Butler BM. 2002. The vacant quarter revisited: late Mississippian abandonment of the Lower Ohio Valley. *American Antiquity* 67(4): 625–641.
- Cohen-Ofri I, Weiner L, Boaretto E, Mintz G, Weiner S. 2006. Modern and fossil charcoal: aspects of structure and diagenesis. *Journal of Archaeological Science* 33(3):428–439.
- Cole F-C. 1951. *Kincaid, a Prehistoric Illinois Metropolis*. Chicago: University of Chicago Press.
- Collard F-X, Blin J. 2014. A review on pyrolysis of biomass constituents: mechanisms and composition of the products obtained from the conversion of cellulose, hemicelluloses and lignin. *Renewable and Sustainable Energy Reviews* 38:594–608.
- Core HA, Côté WA, Day AC. 1979. *Wood structure and identification*. Syracuse, NY: Syracuse University Press.
- Dee MW, Bronk Ramsey C. 2014. High-precision Bayesian modeling of samples susceptible to inbuilt age. *Radiocarbon* 56(1):83–94. doi: [10.2458/56.16685](https://doi.org/10.2458/56.16685).
- Deeyai P, Suphantharika M, Wongsagonsup R, Dangtip S. 2013. Characterization of modified tapioca starch in atmospheric argon plasma under diverse humidity by FTIR spectroscopy. *Chinese Physics Letters* 30(1):018103.
- Emerson JN. 1943. *Final Excavation Report of M X O 10 A Conical-Truncate Mound. The Kincaid*

- Site. Unpublished manuscript. On file at the Center for Archaeological Investigations, Southern Illinois University, Carbondale.
- Fuller GD, Nuuttala EE, Mattoon WR, Miller RB. 1955. Forest trees of Illinois: how to know them. Springfield, IL: Department of Conservation, Division of Forestry.
- Grabner M, Wächter E, Nicolussi K, Bolka M, Sormaz T, Steier P, Wild EM, Barth FE, Kern A, Rudorfer J. 2021. Prehistoric salt mining in Hallstatt, Austria. New chronologies out of small wooden fragments. *Dendrochronologia* 66:125814.
- Hatchfield PB, Koestler RJ. 1987. Scanning electron microscopic examination of archaeological wood microstructure altered by consolidation treatments. *Scanning Microscopy* 1(3):21.
- Hawley Senter F. 1938. Dendrochronology in two Mississippi drainage tree-ring areas. *Tree-Ring Bulletin* 5(1):3–6.
- Hoadley BR. 1990. *Identifying Wood*. Newtown, CT: The Taunton Press.
- Jaggi N, Vij DR. 2006. Fourier transform infrared spectroscopy. In: *Handbook of applied solid state spectroscopy*. New York: Springer. p. 411–450.
- Kaye B. 1995. Conservation of waterlogged archaeological wood. *Chemical Society Reviews* 24(1):35–43.
- Kessler NV. 2021. The distribution of age disparities in conifer charcoal from archaeological structures and applications for tree-ring-radiocarbon dating. *Radiocarbon* 63(6):1607–1628.
- Kessler NV, Butler BM, Brennan TK, Towner RH, Welch PD, Hodgins GWL. 2022. Wiggle-matched red cedar from a pre-monumental occupation at Kincaid Mounds, Illinois, USA. *Tree-Ring Research* 78(2):100–112.
- Kessler NV, Guebard MC, Hodgins GW, Hoedl L. 2022. New tree-ring-radiocarbon dates reveal drought-migration linkage for central Arizona cliff dwelling. *Journal of Archaeological Science: Reports* 41:103289.
- Kessler NV, Hodgins GW, Stambaugh MC, Adair MJ. 2021. Tree-ring-radiocarbon dating at a Late Contact Period Kitkahaki Pawnee site on the Central Great Plains, USA. *Radiocarbon* 63(2):481–497.
- Koerner SD, Grissino-Mayer HD, Sullivan LP, Deweese GG. 2009. A dendroarchaeological approach to Mississippian culture occupational history in Eastern Tennessee, USA. *Tree-Ring Research* 65(1):81–90.
- Lancelotti C, Madella M, Ajithprasad P, Petrie CA. 2010. Temperature, compression and fragmentation: an experimental analysis to assess the impact of taphonomic processes on charcoal preservation. *Archaeological and Anthropological Sciences* 2(4):307–320.
- Liu Q, Wang S, Zheng Y, Luo Z, Cen K. 2008. Mechanism study of wood lignin pyrolysis by using TG–FTIR analysis. *Journal of Analytical and Applied Pyrolysis* 82(1):170–177.
- Manning SW, Birch J, Conger MA, Dee MW, Griggs C, Hadden CS, Hogg AG, Ramsey CB, Sanft S, Steier P. 2018. Radiocarbon re-dating of contact-era Iroquoian history in northeastern North America. *Science Advances* 4(12):eaav0280.
- Manning SW, Dee MW, Wild EM, Ramsey CB, Bandy K, Creasman PP, Griggs CB, Pearson CL, Shortland AJ, Steier P. 2014. High-precision dendro-¹⁴C dating of two cedar wood sequences from First Intermediate Period and Middle Kingdom Egypt and a small regional climate-related ¹⁴C divergence. *Journal of Archaeological Science* 46:401–416.
- Manning SW, Griggs CB, Lorentzen B, Barjamovic G, Ramsey CB, Kromer B, Wild EM. 2016. Integrated tree-ring-radiocarbon high-resolution timeframe to resolve earlier second millennium BCE Mesopotamian chronology. *PLoS One* 11(7):e0157144.
- Manning SW, Kromer B, Ramsey CB, Pearson CL, Talamo S, Trano N, Watkins JD. 2010. ¹⁴C record and wiggle-match placement for the Anatolian (Gordion area) juniper tree-ring chronology ~1729 to 751 cal BC, and typical Aegean/Anatolian (growing season related) regional ¹⁴C offset assessment. *Radiocarbon* 52(4):1571–1597.
- Muller J. 1978. The Kincaid system: Mississippian settlement in the environs of a large site. In: Smith BD, editor. *Mississippian settlement patterns*. New York: Academic Press. p. 269–292.
- Nash SE, Copenheaver CA. 2017. Revival of dendroarchaeology in the Eastern United States. *Dendrochronologia* 100(43):1–3.
- Olsson IU. 1980. ¹⁴C in extractives from wood. *Radiocarbon* 22(2):515–524.
- Pastorova I, Botto RE, Arisz PW, Boon JJ. 1994. Cellulose char structure: a combined analytical Py-GC-MS, FTIR, and NMR study. *Carbohydrate Res.* 262(1):27–47.
- Pearson C, Salzer M, Wacker L, Brewer P, Sookdeo A, Kuniholm P. 2020. Securing timelines in the ancient Mediterranean using multiproxy annual tree-ring data. *Proceedings of the National Academy of Sciences* 117(15):8410–8415.
- Pearson CL, Brewer PW, Brown D, Heaton TJ, Hodgins GW, Jull AT, Lange T, Salzer MW. 2018. Annual radiocarbon record indicates 16th century BCE date for the Thera eruption. *Science Advances* 4(8):eaar8241.
- Pursell C CO. 2016. *Afterimages of Kincaid Mounds* [PhD dissertation]. Carbondale: Southern Illinois University.
- Ramer B. 1979. The technology, examination and conservation of the Fayum portraits in the Petrie Museum. *Studies in Conservation* 24(1):1–13.
- Reimer PJ, Austin WEN, Bard E, Bayliss A, Blackwell PG, Bronk Ramsey C, Butzin M,

- Cheng H, Edwards RL, Friedrich M, et al. 2020. The IntCal20 Northern Hemisphere Radiocarbon Age Calibration Curve (0–55 cal kBP). *Radiocarbon* 62(4):725–757. doi: [10.1017/RDC.2020.41](https://doi.org/10.1017/RDC.2020.41).
- Schaefer K, Mills DJ. 2017. The application of organic coatings in conservation of archaeological objects excavated from the sea. *Progress in Organic Coatings* 102:99–106.
- Sharma RK, Wooten JB, Baliga VL, Lin X, Chan WG, Hajjaligol MR. 2004. Characterization of chars from pyrolysis of lignin. *Fuel* 83(11–12):1469–1482.
- Stahle DW, Wolfman D. 1985. The potential for archaeological tree-ring dating in eastern North America. *Advances in Archaeological Method and Theory* 8:279–302.
- Tasumi M. 2014. Introduction to infrared spectroscopy. In: Mitsuo T, editor. *Introduction to experimental infrared spectroscopy: fundamentals and practical methods*. Sussex, United Kingdom: John Wiley & Sons. p. 33–59.
- Towner RH. 2015. Collecting and caring for tree-ring samples in the southwest. *Advances in Archaeological Practice* 3(4):397–406. doi: [10.7183/2326-3768.3.4.397](https://doi.org/10.7183/2326-3768.3.4.397).
- Traoré M, Kaal J, Cortizas AM. 2016. Application of FTIR spectroscopy to the characterization of archeological wood. *Spectrochimica Acta Part A: Molecular and Biomolecular Spectroscopy* 153:63–70.
- Traoré M, Kaal J, Cortizas AM. 2018. Differentiation between pine woods according to species and growing location using FTIR-ATR. *Wood Science and Technology* 52(2): 487–504.
- Triantafyllou M, Papachristodoulou P, Pournou A. 2010. Wet charred wood: a preliminary study of the material and its conservation treatments. *Journal of Archaeological Science* 37(9): 2277–2283.
- Trompowsky PM, de Melo Benites V, Madari BE, Pimenta AS, Hockaday WC, Hatcher PG. 2005. Characterization of humic like substances obtained by chemical oxidation of eucalyptus charcoal. *Organic Geochemistry* 36(11): 1480–1489.
- Walsh Z, Janeček E-R, Hodgkinson JT, Sedlmair J, Koutsoubas A, Spring DR, Welch M, Hirschmugl CJ, Toprakcioglu C, Nitschke JR. 2014. Multifunctional supramolecular polymer networks as next-generation consolidants for archaeological wood conservation. *Proceedings of the National Academy of Sciences* 111(50): 17743–17748.
- Walsh Z, Janeček E-R, Jones M, Scherman OA. 2017. Natural polymers as alternative consolidants for the preservation of waterlogged archaeological wood. *Studies in Conservation* 62(3):173–183.
- Walsh-Korb Z, Avérous L. 2019. Recent developments in the conservation of materials properties of historical wood. *Progress in Materials Science* 102:167–221.
- Weakly HE. 1943. A tree-ring record of precipitation in western Nebraska. *Journal of Forestry* 41(11):816–819.
- Western CA. 1969. Wood and charcoal in archaeology. In: Higgs ES, Brothwell DR, editors. *Science in archaeology: a survey of progress and research*. New York: Praeger. p. 178–187.
- Wiley GR. 1937. Notes on central Georgia dendrochronology. *Tree-Ring Bulletin* 4(2): 6–8.
- Yu Y, Liu D, Wu H. 2012. Characterization of water-soluble intermediates from slow pyrolysis of cellulose at low temperatures. *Energy & Fuels* 26(12):7331–7339.